Int J Thermophys (2008) 29:1299–1320
DOI 10.1007/s10765-008-0468-z

Determining Thermal Conductivity and Thermal Diffusivity of Low-Density Gases Using the Transient Short-Hot-Wire Method

P. L. Woodfield · J. Fukai · M. Fujii · Y. Takata · K. Shinzato

Received: 26 December 2007 / Accepted: 5 June 2008 / Published online: 8 July 2008

Abstract The transient short-hot-wire method for measuring thermal conductivity and thermal diffusivity makes use of only one thermal-conductivity cell, and end effects are taken into account by numerical simulation. A search algorithm based on the Gauss–Newton nonlinear least-squares method is proposed to make the method applicable to high-diffusivity (i.e., low-density) gases. The procedure is tested using computer-generated data for hydrogen at atmospheric pressure and published experimental data for low-density argon gas. Convergence is excellent even for cases where the temperature rise versus the logarithm of time is far from linear. The determined values for thermal conductivity from experimental data are in good agreement with published values for argon, while the thermal diffusivity is about 10 % lower than the reference data. For the computer-generated data, the search algorithm can return both thermal conductivity and thermal diffusivity to within 0.02 % of the exact values. A one-dimensional version of the method may be used for analysis of low-density gas data produced by conventional transient hot-wire instruments.

Keywords Low-density gas · Thermal conductivity · Thermal diffusivity · Transient short hot wire

P. L. Woodfield (✉) · M. Fujii · K. Shinzato
Research Center for Hydrogen Industrial Use and Storage, National Institute of Advanced Industrial Science and Technology, 744 Mootoka, Nishi-ku, Fukuoka 819-0395, Japan
e-mail: p.woodfield@aist.go.jp

J. Fukai
Department of Chemical Engineering, Graduate School of Engineering, Kyushu University, Nishi-ku, Fukuoka 819-0395, Japan

Y. Takata
Department of Mechanical Engineering Science, Kyushu University, Nishi-ku, Fukuoka 819-0395, Japan

Nomenclature

$a^{i,j}$	Coefficient of algebraic equation for grid point (i, j)
$b^{i,j}$	Source term in discretized equation
c	Specific heat capacity
H	Height of sample container (length of wire)
N	Number of radial or axial grid points or numerical time steps
P	Pressure
q	Heat supplied per unit time per unit length of wire
Q	Heat per unit time per unit volume
r	Radial coordinate
r_0	Wire radius
r_{ij}	Numerical residual for algebraic equation (i, j)
R	Radius of sample container
S	Summation to be minimized
t	Time
T	Temperature
T'	Calculated temperature where the thermal diffusivity has been perturbed (or a required correction to the temperature in the Appendix)
T''	Calculated temperature where the thermal conductivity has been perturbed
x	Coefficient to be determined in least-squares algorithm

Greek

α	Thermal diffusivity
$\delta\alpha$	Small change in thermal diffusivity
$\delta\lambda$	Small change in thermal conductivity
λ	Thermal conductivity
ρ	Density
ψ_i	Difference between calculation and experiment for measurement i

Subscripts

0	Initial or boundary
calc	Calculation
exp	Experiment
r	Radial direction
s	Sample
t	Related to time
w	Wire
z	Axial direction

1 Introduction

The transient hot-wire method is widely considered to be the most accurate technique for thermal-conductivity measurements for both liquids and gases. It has a major

advantage over many other methods in that the required data are collected before the onset of effects of natural convection. Moreover, it is fast, it has a relatively simple analytical working equation, and the technique is well established. However, a number of corrections [1] are necessary to account for differences between the ideal model and the actual instrument. Some of these can be reduced by good design. One important requirement to obtain a linear relationship between the measured temperature rise and the logarithm of time is that the radius of the sample holder, R, be enough for the wire to behave as though it is in a semi-infinite medium. A useful criterion is that the Fourier number $\alpha t/R^2$ be less than about 0.2 [1,2], where t is typically of the order of 1 s or 2 s. This criterion can be met easily for liquids and high-density gases, but for gases where the density is lower than about $0.5\,\mathrm{mol}\cdot\mathrm{L}^{-1}$ (typically $P < 1$ MPa at 25 °C [2,3]), the effect of the outer boundary tends to become severe in instruments of a practical size. For gases where the thermal conductivity is high such as hydrogen and helium, this problem can occur at even higher pressures. Low-density gas measurements are of fundamental importance for theoretical and practical correlation of thermal conductivity. However, for transient hot-wire data, extrapolation to zero density is often done from pressures greater than 1 MPa [2]. This is of some concern, particularly for gases like hydrogen where practically all of the recommended primary reference data has been collected by the transient hot-wire method [4]. Moreover, for refrigerants below the critical pressure, sometimes it is not even possible to extrapolate from high-density vapor data since the fluid becomes a liquid as the pressure is raised [2]. These considerations have motivated a number of authors to propose schemes to make the transient hot-wire method more applicable to measurements in low-density gas [2,5,6].

Analytical corrections are available for the outer boundary effect [1], but the accuracy of the method diminishes as the linear section of the curve becomes shorter and shorter [3]. An alternative is to use large cells for low-pressure work [2]. However, if the same cell is to be employed for high-pressure gas, an unreasonably heavy pressure vessel may be required. Another approach is to use a numerical method to solve the heat conduction equation all the way to the boundary and thus automatically account for the effect of the container wall [5]. Assael et al. [5] reported that for high-diffusivity gas, a one-dimensional finite element solution of the heat conduction equation could yield a more accurate estimation of thermal conductivity than simply following some of the approximate corrections by Healy et al. [1]. The numerical approach appears very promising since all departures from the ideal analytical model can be directly incorporated in the numerical formulation.

Another complication with the conventional transient hot-wire method that can increase the sample volume is related to how to treat the cooling effects near the ends of the cell where the wire connects to the terminals. One of the most successful methods is to use two wires of different lengths (e.g., [6,7]). A different approach is to attach potential taps offset from the ends to measure the voltage across the central region of the wire (e.g., [8]). In either case a long wire is required. About 10 years ago, Fujii et al. [9–11] proposed an alternative method where the two-dimensional unsteady heat conduction equation was solved simultaneously for the wire and sample fluid, automatically accounting for the finite length of the wire. This method has some important advantages over the conventional technique. First, only one cell is required

and it is not necessary to use a long wire. Thus, the method is referred to as the "transient *short*-hot-wire method." The possibility of using a short wire is particularly valuable for reducing the sample size and for measurement of properties of electrically conductive and corrosive fluids where it is necessary to apply a protective coating to the wire [10]. Moreover, the apparatus is simpler than the conventional hot-wire apparatus and all departures from ideal one-dimensional heat conduction are included directly in the numerical model. The main disadvantage with the short-hot-wire method is that additional effort is required to ensure that numerical errors in the simulation do not contribute significantly to the uncertainty in the final estimations of thermal conductivity and thermal diffusivity. However, with the increase in speed and capacity of digital computers, the calculation time required for high-resolution two-dimensional (2D) numerical solutions is diminishing to a point where numerical approaches can become competitive with and even superior to approximate analytical corrections.

In this study we demonstrate that the numerical approach used in the transient short-hot-wire method is a valuable tool to automatically account for the finite tube diameter in addition to the effect of the finite length of the wire. Moreover, we propose a search algorithm to find the thermal conductivity and thermal diffusivity from experimental data where the temperature/log(time) relationship is far from linear.

2 Physical Model

The domain of the model is illustrated in Fig. 1. For a wire of radius r_0 in a cylinder of radius R and height H with heat supplied at q power units per unit length, unsteady heat conduction is given by

$$\rho c \frac{\partial T}{\partial t} = \frac{1}{r}\frac{\partial}{\partial r}\left(r\lambda\frac{\partial T}{\partial r}\right) + \frac{\partial}{\partial z}\left(\lambda\frac{\partial T}{\partial z}\right) + Q \tag{1}$$

$$\begin{aligned} Q &= q/\pi r_0^2 \quad (r \le r_0) \\ &= 0 \quad (r > r_0) \end{aligned} \tag{2}$$

$$T|_{r=R} = T_0 \tag{3}$$

$$T|_{z=0} = T_0 \tag{4}$$

$$\frac{\partial T}{\partial z}|_{z=H/2} = 0 \tag{5}$$

$$T|_{t=0} = T_0 \tag{6}$$

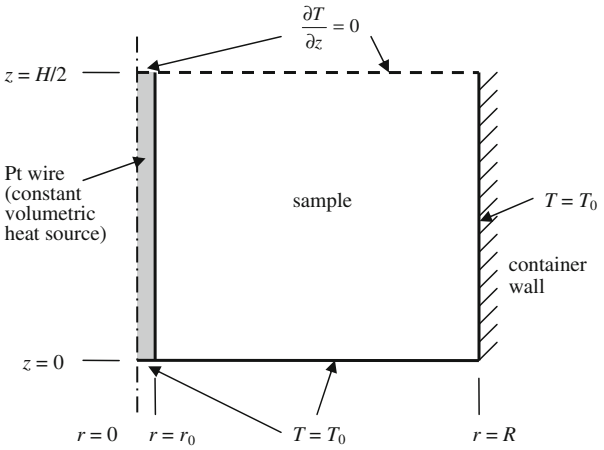

Fig. 1 Short-hot-wire model domain and boundary conditions

$$\lambda|_{r\le r_0} = \lambda_w \quad \lambda|_{r>r_0=\lambda_s} \tag{7}$$

$$\rho c|_{r\le r_0} = \rho_w c_w \quad \rho c|_{r>r_0} = \rho_s c_s \tag{8}$$

In Eq. 2, it is assumed that the power per unit volume is constant and independent of the wire temperature. At the outer wall of the sample container and base of the cylinder and wire, it is assumed that the temperature is fixed at the initial temperature of the cell, as indicated in Eqs. 3 and 4. Symmetry is assumed for half of the domain (Eq. 5). The properties of the gas and wire are assumed to not change with time or temperature.

3 Numerical Solution

3.1 Discretization and Solution of Transient Thermal Field

Equation 1 is discretized using the finite volume method [12] with central differencing for the conduction terms and a fully implicit formulation for the unsteady term. This results in a sparse, linear, diagonally dominant set of equations to be solved. For the present work, the line-by-line tri-diagonal matrix algorithm (TDMA) (see [12]) was used as a preconditioner for a generalized conjugate residuals (GCR) algorithm [13,14]. This combination was found to result in a fast and well-converged solution to the algebraic equations. Details are given in the Appendix.

3.2 Search Algorithm to Find Thermal Conductivity and Thermal Diffusivity

The basic approach used is to start with an initial guess for the properties, solve Eqs. 1–8, and then iteratively adjust the thermal diffusivity and thermal conductivity so that

the solution matches the experimental data. This can be stated as a nonlinear least-squares problem as in Eq. 9 where we need to find λ and α such that the objective function, $S_{\text{non-linear}}$, is minimized;

$$S_{\text{non-linear}} = \sum_{i=1}^{N_{\text{exp}}} \left(T_{\text{exp}\,i} - T_i\,(\lambda, \alpha)\right)^2 = \min \tag{9}$$

In Eq. 9, N_{exp} is the total number of experimental measurements, $T_{\text{exp}\,i}$ is the ith measured temperature, and $T_i\,(\lambda,\alpha)$ is the calculated hot-wire temperature from numerical solution of Eqs. 1–8.

Equation 9 is solved using the Gauss–Newton algorithm for nonlinear least-squares problems (e.g., [15]) with a numerical approximation to the Jacobian. It is worthwhile to outline the method briefly. Let:

$$\psi_i\,(\lambda, \alpha) \equiv T_{\text{exp}\,i} - T_i\,(\lambda, \alpha) \tag{10}$$

Starting with initial guesses, λ_0 and α_0, and using the truncated Taylor series expansion, ψ_{i} can be approximated as

$$\psi_i\,(\lambda, \alpha) \approx \psi_i\,(\lambda_0, \alpha_0) + (\alpha - \alpha_0)\,\frac{\partial \psi_i}{\partial \alpha}|_0 + (\lambda - \lambda_0)\,\frac{\partial \psi_i}{\partial \lambda}|_0 \tag{11}$$

The concept for the Gauss–Newton method is to substitute Eq. 11 into Eq. 9 and then solve the resulting linear least-squares problem to obtain better estimates for α and λ. Iteration ultimately yields the solution to Eq. 9 provided the algorithm converges. For the present study, the gradients in Eq. 11 are approximated numerically by finite differences using small changes in α and λ denoted by $\delta\alpha$ and $\delta\,\lambda$, respectively. This yields

$$\begin{aligned}\psi_i\,(\lambda, \alpha) \approx \psi_i\,(\lambda_0, \alpha_0) + \frac{(\alpha - \alpha_0)}{\delta\alpha}\,(T_i\,(\lambda_0, \alpha_0) - T_i\,(\lambda_0, \alpha_0 + \delta\alpha)) \\ + \frac{\lambda - \lambda_0}{\delta\lambda}\,(T_i\,(\lambda_0, \alpha_0) - T_i\,(\lambda_0 + \delta\lambda, \alpha_0))\end{aligned} \tag{12}$$

For conciseness, let $T_i = T_i\,(\lambda_0, \alpha_0)$, $T_i' = T_i\,(\lambda_0, \alpha_0 + \delta\alpha)$, $T_i'' = T_i\,(\lambda_0 + \delta\lambda, \alpha_0)$, and substitute Eq. 12 into Eq. 9. This results in a linear least-squares problem given by

$$S_{\text{linear}} = \sum_{i=1}^{N\,\text{exp}} \left(\left(T_{\text{exp}\,i} - T_i\right) - x_\alpha\left(T_i' - T_i\right) - x_\lambda\left(T_i'' - T_i\right)\right)^2 = \min \tag{13}$$

The unknowns, x_α and x_λ, in Eq. 13 are defined in terms of the unknown α and λ as

$$x_\alpha = \frac{\alpha - \alpha_0}{\delta\alpha} \qquad x_\lambda = \frac{\lambda - \lambda_0}{\delta\lambda} \tag{14}$$

Thus, to solve Eq. 9, the following algorithm is employed:

1. Guess α and λ
2. Solve Eq. 1 to give the volume-averaged wire temperature: $(T_j, t_{\mathrm{calc}\,j})\, j = 1, N_{\mathrm{calc}}$
3. Using the calculated result, interpolate to find temperatures at the times when experimental data were collected: $(T_i, t_{\mathrm{exp}i})i = 1, N_{\mathrm{exp}}$
4. Set $\alpha' = \alpha + \delta\alpha$ and solve Eq. 1 again but with α' and λ and interpolate: $(T_i', t_{\mathrm{exp}i})$
5. Set $\lambda' = \lambda + \delta\lambda$ and solve Eq. 1 again but with α and $\lambda'$and interpolate: $(T_i'', t_{\mathrm{exp}i})$
6. Find x_α and x_λ such that S_{linear} given by Eq. 13 is minimized
7. Set the new values for λ and α such that

$$\lambda^{\mathrm{new}} = \lambda + x_\lambda \delta\lambda \quad \alpha^{\mathrm{new}} = \alpha + x_a \delta\alpha$$

8. Repeat steps 2–7 until the result converges

For the present study, $\delta\alpha$ and $\delta\lambda$ are taken to be 1 % of the current estimated values for α and λ, respectively. Equation 13 (i.e., step 6) is solved with the linear least-squares method using Gram–Schmidt ortho-normalization and Q–R factorization. With initial guesses for α and λ within ± 50 % of the actual values, the above algorithm is found to converge by about 5 or 6 iterations. If the initial guesses are within ± 5 %, only 2 iterations may be required.

4 Test Results

4.1 Computer-Generated Data for Hydrogen Gas at 0.1013 MPa

Computer-generated data provide a useful basic test since the exact solutions for the thermal conductivity and thermal diffusivity are known. Hydrogen at atmospheric pressure in a small sample container is a severe test for the transient-hot-wire method since the thermal diffusivity is quite large and the heating effect soon reaches the wall of the container. The approach adopted here is to create some data for the wire temperature by solving Eq. 1 and then starting from different initial guesses; the procedure outlined above in Sect. 3.2 is applied to test if the algorithm will return the correct values for α and λ. The circles in Fig. 2 show some computer-generated test data. Fifty data points were used, evenly spaced in time from 0.02 s to 1 s. Note that the data are not linear and that a steady state is reached due to the finite size of the sample vessel. This behavior is typical for a low-density gas [1,2].

The results for computer-generated data are shown in Fig. 2 and Table 1. Note that the same grid spacing was used for generating the data and for analysis in this example ($N_r \times N_z = 200 \times 25$). Therefore, in principle, it should be possible to return to the original thermal conductivity and thermal diffusivity, to the order of the computational rounding error. It is clear from Table 1 that the algorithm works very well, even from a rather poor initial guess. In fact, for the case considered in Fig. 2, the final converged value for the present method was found to be insensitive to the initial guess and also to the sizes of $\delta\alpha$ and $\delta\lambda$ used in steps 4 and 5 of the algorithm. The main effect of the

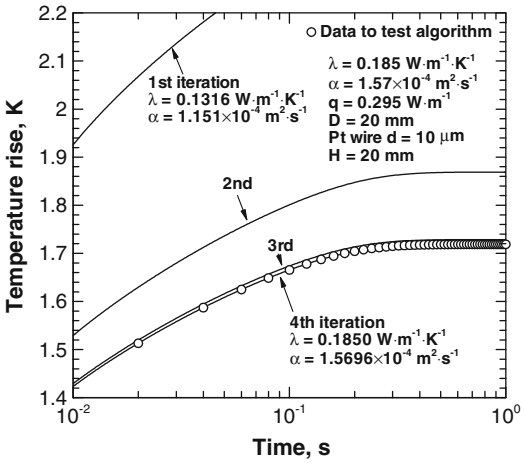

Fig. 2 Testing the present algorithm using computer-generated data for hydrogen gas at 0.1013 MPa, 25 °C. The temperature rise is for the volume-averaged wire temperature

Table 1 Search algorithm convergence ($\lambda = 0.185\,\mathrm{W\cdot m^{-1}\cdot K^{-1}}$, $\alpha = 1.57\times10^{-4}\ \mathrm{m^2\cdot s^{-1}}$)

	Thermal conductivity ($\mathrm{W\cdot m^{-1}\cdot K^{-1}}$)	Thermal diffusivity ($10^{-4}\,\mathrm{m^2\cdot s^{-1}}$)	Thermal conductivity error (%)	Thermal diffusivity error (%)
Initial guess	0.085	1.0	54	36
1st iteration	0.1316223	1.150692	29	27
2nd iteration	0.1700767	1.385250	8.1	12
3rd iteration	0.1839467	1.541626	0.57	1.8
4th iteration	0.1850046	1.569681	0.0025	0.020
5th iteration	0.1849999	1.570002	0.000025	0.00013
6th iteration	0.1850000	1.570000	0.00000026	0.00000087

initial guess is that a poor guess requires a larger number of iterations for the solution to converge. It is worth mentioning, however, that the initial guesses should be of the correct order of magnitude since it is possible for the linear approximation (Eq. 13) to yield negative values for the properties if the thermal diffusivity estimate is much too large.

4.2 Numerical Grid Convergence

Since both the test case and the search algorithm used the same numerical grid, the convergence shown in Table 1 only demonstrates that the algorithm works effectively. It does not give a true indication of the numerical error in the method. Provided the model is physically correct and the solution converges properly, the main source of numerical error is in the numerical discretization of Eq. 1. In principle, it is always possible to reduce the numerical error to a value much smaller than the experimental error by using progressively finer computational grids and smaller time steps. The practical limit to numerical accuracy is actually determined by the available calculation time. Since we must solve Eq. 1 many times, we are practically limited to the finest grid that can be solved in a few minutes. Thus, the numerical accuracy of the present method

Table 2 Grid convergence for computer-generated test case ($\lambda = 0.185 \mathrm{W \cdot m^{-1} \cdot K^{-1}}$, $\alpha = 1.57 \times 10^{-4} \mathrm{m^2 \cdot s^{-1}}$)

Grid $N_r \times N_z$	Time N_t	First (or smallest)			λ ($\mathrm{W \cdot m^{-1} \cdot K^{-1}}$)	λ (error) (%)	α ($10^{-4} \mathrm{m^2 \cdot s^{-1}}$)	α(error) (%)	Calc. time (min)
		$\Delta r/r_{\mathrm{wire}}$	$\Delta z/r_{\mathrm{wire}}$	Δt (μs)					
133 × 18	800	0.6	7.5	75	0.18448	0.28	1.5732	0.20	2
200 × 25	1,200	0.4	5.0	50	0.18477	0.12	1.5716	0.10	10
300 × 38	1,800	0.27	3.75	38	0.18491	0.05	1.5710	0.06	46
450 × 50	2,700	0.18	2.5	10	0.18497	0.016	1.5697	0.02	180

can improve if a faster computer is used or more computation time is available for data processing. In any case, for high-precision work it is important to *demonstrate* the grid convergence and not rely too heavily on past experience since it is very easy for numerical errors to appear. We propose that this be done by tabulating the thermal conductivities and thermal diffusivities determined using different grid spacing as illustrated in Table 2.

For all cases in Table 2 the test data were generated using a 600×75 grid ($N_r \times N_z$). The smallest grid sizes, Δr and Δz, are quite important since the steepest radial temperature gradients occur next to the wire and the steepest axial temperature gradients occur at $z = 0$. Therefore, they are also given in the table. Starting with the smallest values, geometric progressions are used to determine the grid spacing for the entire domain. Initially small time steps are required (Δt in Table 2) but this becomes less important as time progresses, so it is also permissible for the time steps to increase geometrically. This observation was verified by a numerical experiment. The number of grid points in the r-direction needs to be more than in the z-direction due to the steep temperature gradient next to the wire.

The calculation times given in Table 2 are wall-clock times for six iterations of the present method on a Pentium D personal computer with a clock speed of 3 GHz. (Note that six iterations imply that Eq. 1 is solved 18 times.) The convergence criterion for each time step was a reduction in the residual-squared norm of seven orders of magnitude from its value at the start of the calculation. Two seconds of data were produced for each case to compare with 50 points evenly spaced in the period from 0.02 s to 1 s.

In Table 2, the number of grid points in each direction, N_r, N_z, and time steps, N_t, are increased by a factor of 1.5 with each refinement. For the present numerical scheme, this results in a reduction of the numerical error of about one-half but an increase in the required time for calculation by a factor of about five. Based on Table 1, we can see that the number of iterations, and hence the calculation time, can be reduced by using better initial guesses. This indicates that in practice it may be best to use a coarse grid first to obtain a reasonably accurate estimate before applying the fine grid. In any case, Table 2 indicates that a numerical error of the order of 0.05 % may be achieved in less than 1 h using the present technique on a fairly standard personal computer.

It is also worth noting that using the present numerical scheme, the difference between consecutive grid refinements in Table 2 is of the same order of magnitude or slightly larger than the absolute error. This is important since for experimental data

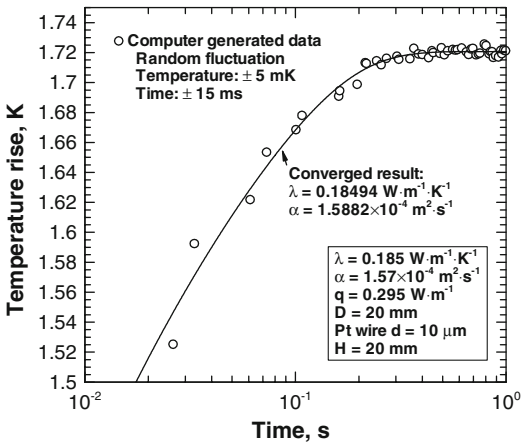

Fig. 3 Application of the present technique to computer-generated data with random noise

Table 3 Grid convergence for test case with noise ($\lambda = 0.185\ \mathrm{W \cdot m^{-1} \cdot K^{-1}}, \alpha = 1.57 \times 10^{-4} \mathrm{m^2 \cdot s^{-1}}$)

Grid $N_r \times N_z$	Time N_t	First (or smallest)			λ ($\mathrm{W \cdot m^{-1} \cdot K^{-1}}$)	λ (error) (%)	α ($10^{-4}\,\mathrm{m^2 \cdot s^{-1}}$)	α (error) (%)
		$\Delta r/r_{\mathrm{wire}}$	$\Delta z/r_{\mathrm{wire}}$	$\Delta t\,(\mu\mathrm{s})$				
133 × 18	800	0.6	7.5	75	0.18449	0.28	1.5894	1.2
200 × 25	1,200	0.4	5.0	50	0.18480	0.11	1.5889	1.2
300 × 38	1,800	0.27	3.3	33	0.18494	0.03	1.5882	1.0

we do not know the exact values of the thermal conductivity and thermal diffusivity. Thus, the difference between consecutive grid refinements (using $1.5N_r$, $1.5N_z$, $1.5N_t$ at each refinement) gives a reasonable indication of the numerical error of the present numerical scheme.

4.3 Effect of Noise in Data

To simulate the effect of noise in the data, the above calculations were repeated with a random fluctuation added to each computer-generated data point. Time measurements were assumed to have a 2σ uncertainty of ± 15 ms and temperature readings an uncertainty of ± 5 mK. The random fluctuations were taken to be normally distributed and were produced using the Box–Muller method.

Figure 3 shows the test data and final converged result using the present method applied to the data containing noise. The time component of the random fluctuation has a large influence on the data at small values of t, while at large values of t, the uncertainty in the temperature is more important. Table 3 shows the grid convergence. Comparing Tables 2 and 3, it is clear that the noise had little effect on the value of thermal conductivity. Thermal diffusivity on the other hand converged to a value about 1 % higher than the true value of $1.57 \times 10^{-4}\,\mathrm{m^2 \cdot s^{-1}}$.

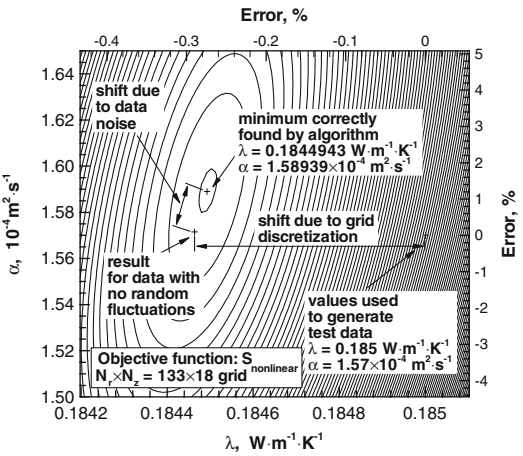

Fig. 4 Contours of the nonlinear objective function (Eq. 9) for data including random noise

A possible concern with application of the present technique to data containing noise is that the noise may introduce local minima in the objective function. To investigate this possibility, the objective function for the 133 × 18 grid in Table 3 is plotted in Fig. 4. It is evident in this figure that only one minimum appeared and it was correctly found by the present algorithm. For this example, the main effect of the noise was to shift the location of the minimum rather than introducing new minima. Another interesting observation from Fig. 4 is that the objective function has a sharp minimum with respect to λ but a shallow minimum with respect to α. Also, the error in the estimate for λ is due mostly to the grid discretization, while on the other hand the random noise is largely responsible for the error in the thermal-diffusivity estimate for the case plotted in Fig. 4. Thus, we may conclude that thermal diffusivity is more susceptible to the influence of noise than thermal conductivity.

4.4 Importance of Boundary Conditions for Low-Density Gas Analysis

Since the boundary condition at $r = R$ is important for high-diffusivity fluids, we should expect that the boundary conditions at the bottom and top of the cylinder will also be important. Figure 5 shows steady-state distributions of the temperature rise for three different boundary conditions on the lower part of the cylinder. Figure 5a is the same boundary condition as specified by Eq. 4. In Fig. 5b an isothermal boundary is used for $r < 1$ mm and an insulated boundary for $r > 1$ mm at the bottom of the cylinder. In Fig. 5c calculations were performed where the platinum wire is supported by a 2 mm diameter copper wire that extends 3 mm from the lower wall. In all three cases the length of the platinum wire is the same. Clearly the temperature distributions within the sample are different among the three cases. Generally, the gas temperatures are the highest for the case shown by Fig. 5b and lowest for Fig. 5a.

For the present study, the important consideration is the effect that the different boundary conditions have on the volume-averaged wire temperature. This is shown in Fig. 6. During the first 0.02 s it is difficult to distinguish between the three cases.

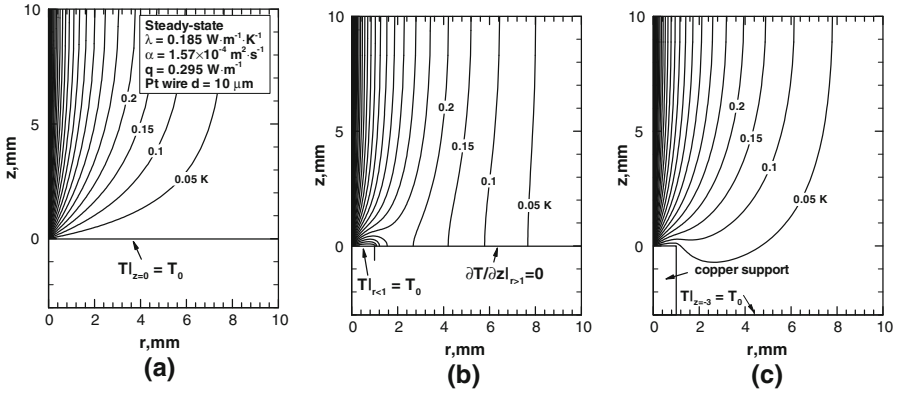

Fig. 5 Steady-state temperature distributions for different boundary conditions in low-density H_2 gas (**a**) Isothermal boundary at $z = 0$, (**b**) Insulated lower boundary for $r > 1$ mm, and (**c**) 2 mm diameter copper supporting wire

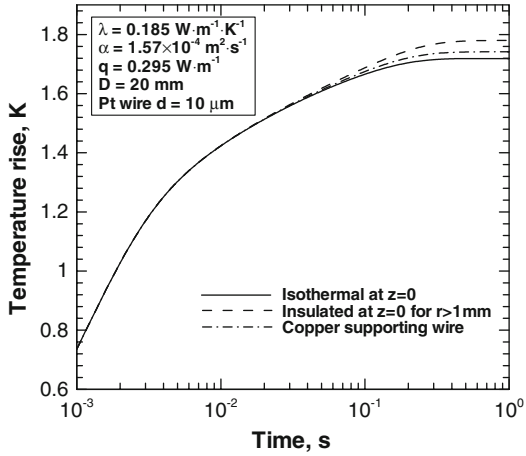

Fig. 6 Calculated volume-averaged wire temperature rise for the cases shown in Fig. 5

This should be expected since it will take time for the heating effect of the wire to reach beyond a radial distance of 1 mm where the three cases become different. However, by about 0.1 s the differences between the curves in Fig. 6 are quite clear and reach a maximum of about 0.06 K corresponding to the steady-state condition. If data generated using the boundary conditions shown in Fig. 5c are analyzed using the present method with the boundary condition given by Eq. 4, the thermal conductivity is estimated to be about 1.3 % lower than the true value. Moreover, the thermal diffusivity is estimated to be about 16 % lower than the true value. Therefore, it is essential that boundary conditions at the top and bottom of the sample holders are realistic representations of the actual instrument for the present technique to be applicable for low-density gas analysis.

Table 4 Instrument dimensions (Sun et al. [16])

Material	Wire diameter	Short-wire length	Long-wire length	Cylinder diameter
Platinum	13.06 μm	28.26 mm	85 mm	10.0 mm

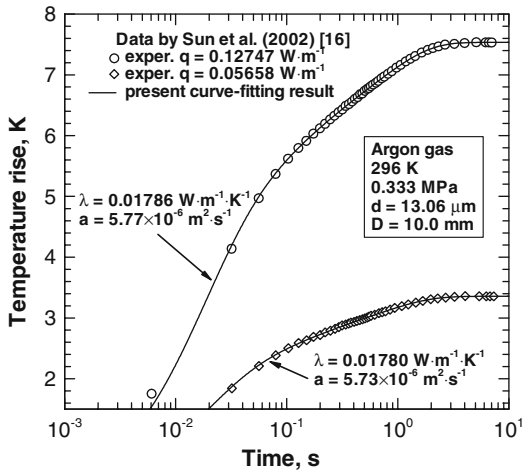

Fig. 7 Present algorithm applied to experimental data for low-density argon gas [14]

4.5 Experimental Data for Argon Gas at 0.333 MPa

A representative case published by Sun et al. [16] was used to verify the applicability of the present method to actual experimental data. In their work, they reported data that were already corrected for end effects. Such data can still be used in the present procedure simply by comparison with the calculated temperatures at the center of the wire. In fact, the one-dimensional solution should be sufficient in this case (which incidentally requires negligible computer time). However, as an additional check, we retained the full 2D solution and made use of the wire center temperature. The geometry for the case of Sun et al. [16] is given in Table 4. Calculations were performed for both the long- and short-wire lengths and were found to be in good agreement with the one-dimensional case. This indicates that the correction method for end effects used by Sun et al. was effective, and it shows that the one-dimensional numerical solution is suitable for analysis of data from conventional transient hot-wire instruments.

Figure 7 compares the present calculation with the experimental measurements for two different powers supplied to the wire. As can be seen, departures from linearity for $t < 0.1$ s and for $t > 2$ s are well captured by the present model. Table 5 indicates that the grid convergence for the thermal conductivity is of the order of 0.06 % while for thermal diffusivity it is of the order of 0.2 %. Sun et al. [16] did not give the thermal diffusivity separately for the two cases given in Table 5, but rather they reported a corrected value based on both results.

Table 6 compares the present results with some reference data for argon from the literature. The thermal conductivity agrees with literature values to within about 0.3 %

Table 5 Grid convergence for analysis of data from Sun et al. [16]

Temperature (K)	Power ($W \cdot m^{-1}$)	Grid $N_r \times N_z$	Time N_t	First (or smallest)			λ ($W \cdot m^{-1} \cdot K^{-1}$)	α ($10^{-6}\, m^2 \cdot s^{-1}$)
				$\Delta r/r_{wire}$	$\Delta z/r_{wire}$	Δt (μs)		
299.161	0.05658	200×25	1200	0.4	5.0	50	0.01779	5.744
		300×38	1,800	0.27	3.75	38	0.01780	5.733
		Values determined by Sun et al. [16]:					0.01777	(6.262)[a]
302.787	0.12747	200×25	1200	0.4	5.0	5.	0.01785	5.781
		300×38	1,800	0.27	3.75	38	0.01786	5.770
		Values determined by Sun et al. [16]					0.01788	(6.262)[a]

[a] Reported value for thermal diffusivity [16] is based on both readings corrected to $T = 296.63\,K$

Table 6 Comparison of present estimates with argon reference data

T (K)	P (MPa)	λ ($W \cdot m^{-1} \cdot K^{-1}$)			α ($10^{-6}\, m^2 \cdot s^{-1}$)		
		Present	Ref. [18]	Ref. [17]	Present	Ref. [18,19][a]	Ref. [17]
299.161	0.333	0.01780	0.01787	0.01775	5.733	6.361	6.316
302.787	0.333	0.01786	0.01805	0.01792	5.770	6.504	6.458

[a] λ from [18], ρ and c_p from [19] to determine the thermal diffusivity

for Ref. [17] and 1 % for Ref. [18]. The thermal diffusivity values are about 8 % lower than those reported by Sun et al. listed in Table 5 and about 10 % lower than the reference data shown in Table 6. The poorer agreement for thermal diffusivity can be explained in part by the strong sensitivity of the hot-wire method for determining thermal diffusivity to small changes in the absolute values of the measured temperatures.

4.6 Natural Convection Issues

The present method is powerful in that the measured temperature data do not need to fall on a straight line when plotted against the logarithm of time. However, this may raise concerns with respect to natural convection since one method of eliminating natural convection is to discard the data that depart from a straight line by a certain percentage [8]. Thus, we need to confirm that the present method will not mistake natural convection effects for outer boundary effects (which may appear similar on a plot of temperature rise versus the logarithm of time). To do this, we make use of some data published for liquid toluene [8] where the effects of natural convection can be observed clearly.

The circular symbols in Fig. 8 show measurements for toluene by Nagasaka and Nagashima [8] using a 15 μm platinum hot wire. End effects are experimentally removed from the data by attaching potential taps part way along the wire. As in Sect. 4.3 it is assumed that the temperature given from experiment is equivalent to the wire center temperature for the present method. As can be seen from the circular symbols

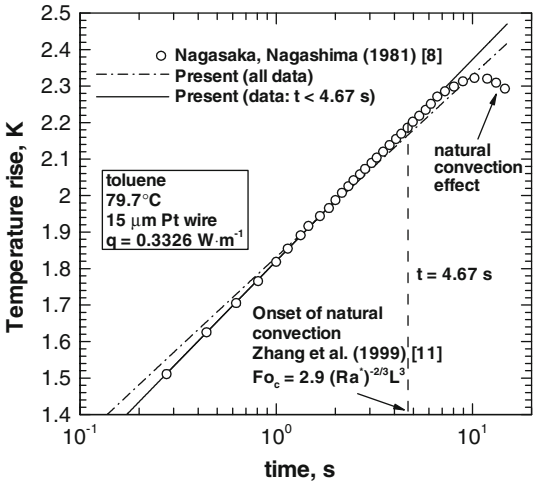

Fig. 8 Application of present method to experimental data for toluene [8]. Data influenced by natural convection must be discarded based on criterion such as given by Zhang et al. [11]

in Fig. 8, natural convection causes a severe departure from the straight line such that the wire temperature even begins to decrease after about 10 s. Zhang et al. [11] give a useful criterion for avoiding natural convection which is marked by the vertical dashed line. For this particular case, using Zhang's criterion, data beyond 4.67 s, should be discarded as possibly being influenced by natural convection. The solid line shows the result of applying the present method only to the data for times less than 4.67 s, while the dashed–dotted line represents application of the present method to all data including that influenced by natural convection. Clearly the dashed–dotted line does not agree with the experimental data. This is in contrast to Fig. 7 where the present calculation agrees well with the full trend of the data. Thus, we may suspect that if the converged result does not agree with the measured data then the data have been influenced by another phenomenon (such as natural convection in this case) that has not been included in the model (Eq. 1).

It is worth mentioning that natural convection effects decrease dramatically as the density of the gas is reduced [3,6]. In fact, this principle is usually used to justify neglecting natural convection effects in the steady hot-wire method for measuring thermal conductivity. Figure 8 shows a case where the issue is clear-cut. A more subtle distinction may occur for hydrogen or argon gas in a small thermal conductivity cell at moderate pressures. In such cases it may be necessary to rely on Rayleigh number-based criteria [11] to discard spurious data. Alternatively, analysis could be repeated using part of the data set, excluding data for larger values of t, which should be affected the most by natural convection. Low sensitivity to the time range of data selected for analysis could be an additional indication for the absence of natural convection effects.

4.7 Comparison with Classical Analytical Analysis

For low-density gas the classical analytical analysis requires a number of corrections (see Refs. [1,3,5]). Therefore, rather than entering into a discussion of the relative

Table 7 Comparison of present estimates for toluene with conventional method estimates

T (°C)	λ ($W \cdot m^{-1} \cdot K^{-1}$)			α ($10^{-8}\, m^2 \cdot s^{-1}$)		
	Present	Analytical	Ref. [20]	Present	Analytical	Ref. [20,21][a]
79.7	0.1104	0.1104	0.1150	5.03	4.98	7.58

[a] λ from [20], ρ and c_p from [21] to determine the thermal diffusivity.

importance of the various analytical corrections, we will just consider the simple case of liquid toluene, which can behave almost ideally in a well-designed instrument [8]. This test also demonstrates the applicability of the present method to standard transient hot-wire data. Table 7 gives analysis of the toluene data [8] shown in Fig. 8 for $t < 4.67$ s. For thermal conductivity, the present method is in agreement with the classical analytical analysis (without corrections) to better than 0.1 %. Thermal diffusivity on the other hand differs by about 1 % for the two methods.

Unfortunately, neither the present nor the analytical method shows good agreement with the reference data for the thermal diffusivity of toluene. This may be explained partly by the fact that thermal diffusivity is very sensitive to the absolute value of the temperature rise as mentioned earlier, and the data shown in Fig. 8 were scanned from a printed figure. It is conceivable that additional uncertainty due to the printing may have influenced the quality of the data. Nevertheless, it is encouraging that the present method is in good agreement with the classical analytical analysis for the same data set.

4.8 Effect of Variable Fluid Properties

In the algorithm outlined in Sect. 3.2 we have assumed that α and λ are constant but in reality they will be a function of the fluid temperature. In the traditional transient hot-wire method, by treating thermal conductivity and volumetric heat capacity as linear functions of temperature, Healy et al. [1] showed that variation in fluid properties could be treated by re-specifying the temperature, T_r, at which the properties are measured;

$$T_r = \frac{1}{2}\{\Delta T\,(t_1) + \Delta T\,(t_2)\} + T_0 \tag{14}$$

where T_0 is the bath temperature, $\Delta T(t_1)$ is the temperature rise of the wire at time t_1 and the data used to specify the slope were collected in the time range from t_1 to t_2. For the steady-state hot-wire method the average of the wire temperature and the outer wall temperature is sometimes used [3]. Using similar notation to Eq. 14, the corrected bath temperature for the steady-state hot-wire method is

$$T_{rSS} = \frac{1}{2}\Delta T\,(t_2) + T_0 \tag{15}$$

where t_2 is a value of time large enough for steady state to be reached. To test if either of the above "bath temperature corrections" is useful in the present method,

Table 8 Effect of variable gas properties in the present model

Condition	λ ($W \cdot m^{-1} \cdot K^{-1}$)	Error (%)	α ($10^{-4} m^2 \cdot s^{-1}$)	Error (%)
Variable property simulation	0.18544	–	1.5767	–
Constant properties at T_0	0.185	0.24	1.57	0.42
Constant properties at T_r	0.18577	0.18	1.5844	0.49
Constant properties at T_{rss}	0.18541	0.016	1.5777	0.06

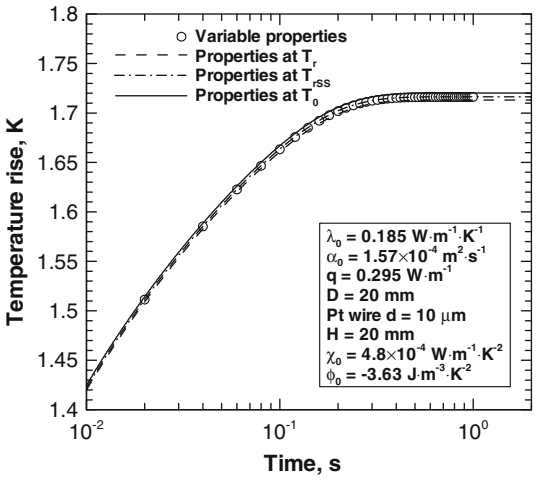

Fig. 9 Effect of variable fluid properties (hydrogen at 25 °C, 0.1013 MPa)

we simulated the temperature rise of the wire using hydrogen gas properties that vary linearly with temperature according to

$$\lambda = \lambda_0 + \chi_0 (T - T_0) \tag{16a}$$

$$\rho c = \rho_0 c_0 + \phi_0 (T - T_0) \tag{16b}$$

For hydrogen gas at atmospheric pressure we used $\chi_0 = 4.8 \times 10^{-4} W \cdot m^{-1} \cdot K^{-2}$ and $\phi_0 = -3.63 J \cdot m^{-3} \cdot K^{-2}$ (from Ref. [17]). Taking the simulated temperatures, we recalculated the thermal conductivity and thermal diffusivity using the present technique. The results are shown in Table 8 with a comparison of the expected results for T_r and T_{rSS} using Eqs. 14 and 15, respectively. For simplicity we used the volume-averaged wire temperature to evaluate $\Delta T(t_1)$ and $\Delta T(t_2)$ in Eqs. 14 and 15. Clearly from Table 8, for this particular example, the simple average of final wire temperature and the wall temperature (Eq. 15) gives the best correction to the bath temperature. This result is confirmed in Fig. 9 which shows constant property simulations at three temperatures T_r, T_{rSS}, and T_0 and the variable property simulation. In Fig. 9, the result for properties evaluated at T_{rSS} (dashed–dotted line) is in the best agreement with the variable property simulation (symbols).

The reason for the suitability of Eq. 15 to the low-pressure hydrogen data is probably because many of the data in Fig. 9 are close to the steady-state condition. We also performed a similar numerical experiment for hydrogen gas at 100 MPa. In the

high-pressure case the data form a straight line when plotted against the logarithm of time, and consistent with the analysis of Healy et al. [1], Eq. 14 provides a slightly more accurate bath temperature correction than Eq. 15. Therefore, for low-pressure gas data using the present technique we tentatively recommend Eq. 15.

5 Range of Applicability for Present Technique

The main purpose of the method proposed in this article is to extend the applicability of the transient short-hot-wire method to low-density gases. In the above sections we have demonstrated that the present approach is suitable for low-density gas and also for liquids provided data influenced by natural convection can be excluded from the analysis. Numerical limitations in the algorithm are important, but we have found that the present technique will converge even for data where the underlying model is not appropriate (e.g., the dashed–dotted line in Fig. 8). Therefore, it is important to note that the method is only applicable in so far as the model outlined by Eqs. 1–8 is a valid representation of the actual instrument and sample fluid. The model will need modification for gas pressures significantly lower than atmospheric where a temperature discontinuity may occur at the wire surface. Data strongly influenced by natural convection, particularly near the critical point, may be difficult to analyze with the present technique. Problems where fluid properties vary sharply may need special treatment. Also, problems where the effect of thermal radiation by the fluid is significant will require a radiation model. The geometry and boundary conditions of the actual cell must also be consistent with Fig. 1 as demonstrated in Sect. 4.4. The power of the present technique lies in the fact that the underlying model can be modified to account for all kinds of situations. Numerical issues will ultimately restrict the range of applicability of the method if the chosen model is too complicated to be solved accurately within a short time.

6 Conclusions

1. The proposed search algorithm to determine thermal conductivity and thermal diffusivity works well for low-density gas data.
2. The magnitude of the numerical error depends on the finest computational grid for which the transient thermal field can be calculated within a few minutes.
3. With the present scheme, the numerical error due to discretization can be reduced to less than 0.1 % of the determined thermal conductivity for a total calculation time of less than 1 h on a personal computer.
4. The present method when combined with a real instrument is more accurate for determining thermal conductivity than for thermal diffusivity.
5. The estimate for thermal diffusivity is more sensitive to noise in the data than thermal conductivity.
6. When applying the present method to data that may have been influenced by natural convection, the departure from a straight line should not be used as the criterion for detecting the onset of natural convection. Rather, an empirical criterion such as that given by Zhang et al. [11] should be applied for discarding data points.

7. For liquids and high-density gases, the present method is expected to agree with the classical analytical analysis to better than 0.1 % for determination of thermal conductivity.
8. The proposed search algorithm (Sect. 3.2) can be used for both the short-hot-wire method and for analysis of data from the conventional transient hot-wire instruments. Conventional data only require that the 1-D unsteady heat conduction equation be solved.

Acknowledgments This research has been conducted as a part of the "Fundamental Research Project on Advanced Hydrogen Science" funded by the New Energy and Industrial Technology Development Organization (NEDO).

Appendix

Simplified Minimum Residuals Algorithm for Solving Discretized Equations for the Short-Hot-Wire Problem

The practical success of the present short-hot-wire method rests on the ability to solve the resulting equations quickly and accurately. Since subtle variations in the formulation for the matrix solver can have a large influence on the calculation time, it is worthwhile giving attention to the details of a method that the first author of this article found successful for this problem.

The algebraic equation for any temperature $T_{i,j}$ at the grid point (i, j) can be written in the form of

$$a_{\mathrm{p}}^{i,j} T_{i,j} = a_{\mathrm{w}}^{i,j} T_{i-1,j} + a_{\mathrm{e}}^{i,j} T_{i+1,j} + a_{\mathrm{s}}^{i,j} T_{i,j-1} + a_{\mathrm{n}}^{i,j} T_{i,j+1} + b^{i,j} \tag{A1}$$

The subscripts p, w, e, s, and n stand for main point, west, east, south, and north, respectively (following the naming convention in Ref. [12]), where north is the positive z-direction and east is the positive radial direction. The set of equations is solved iteratively for each time step. If $T_{i,j}^{\mathrm{current}}$ is the current estimate for $T_{i,j}$, then the residual, r_{ij} is defined by

$$r_{i,j} \equiv a_{\mathrm{w}}^{i,j} T_{i-1,j}^{\mathrm{current}} + a_{\mathrm{e}}^{i,j} T_{i+1,j}^{\mathrm{current}} + a_{\mathrm{s}}^{i,j} T_{i,j-1}^{\mathrm{current}} + a_{\mathrm{n}}^{i,j} T_{i,j+1}^{\mathrm{current}} + b^{i,j} - a_{\mathrm{p}}^{i,j} T_{i,j}^{\mathrm{current}} \tag{A2}$$

If we substitute $T_{i,j} = T_{i,j}^{\mathrm{current}} + T'_{i,j}$ in Eq. A1 where $T'_{i,j}$ is the required correction to satisfy Eq. A1 then we have

$$r_{i,j} = a_{\mathrm{p}}^{i,j} T'_{i,j} - a_{\mathrm{w}}^{i,j} T'_{i-1,j} - a_{\mathrm{e}}^{i,j} T'_{i+1,j} - a_{\mathrm{s}}^{i,j} T'_{i,j-1} - a_{\mathrm{n}}^{i,j} T'_{i,j+1} \tag{A3}$$

Now assume we have n different estimates at which correction might be required and assume that $T'_{i,j}$ can be approximated by a linear combination of these estimates (or so-called search directions),

$$\{T'\} \approx x_1 \{T'_{\mathrm{search}1}\} + x_2 \{T'_{\mathrm{search}2}\} + \cdots + x_n \{T'_{\mathrm{search}n}\} \tag{A4}$$

Here the curly brackets { } are used to indicate a vector containing all components, $T'_{i,j}$. The principle of minimum residual methods is to substitute Eq. A4 into Eq. A3 and then solve for x_1 to x_n such that the sum of the squares of the residuals $r_{i,j}$ is minimized. The search directions can be anything at all; however, if one of them happens to be approximately a multiple of the unknown $\{T'\}$, then convergence is very fast. For this reason it may be helpful to think of the search directions as 'estimates' for $\{T'\}$ as mentioned above. Ideally the search directions should be approximately orthogonal to each other. Often as a result of the way they are generated, the search directions belong to the so-called Krylov subspace [14]. In practice, for efficiency, generation of search directions, the above substitution, and solution of the least-squares problem are intertwined in the particular minimum residual algorithm.

The generalized conjugate residual (GCR) method [13] uses multiple search directions which are saved and automatically generated as the algorithm progresses. However, any stationary iterative method (e.g., Gauss–Seidel iterations, line-by-line tri-diagonal matrix algorithm (TDMA)) can be used for generating new search directions. This approach is called preconditioned GCR in Wesseling's text [14] and was used for the present work. After testing a few alternatives, it was found that generating just one search direction using the TDMA method was effective for the present problem. For only one search direction, the GCR algorithm can be simplified greatly. Thus, rather than giving the full algorithm we will explain the simplified version.

1. Generate search direction using TDMA

This can be done as follows:

$$\left\{T^{\text{search}}\right\} = \left\{T^{\text{current}}\right\}$$

DO (about 10 times)

DO $(i = 1, N_i)(j = 1, N_j)$

$$c_{i,j} = b_{i,j} + a_s^{i,j} T_{i,j-1}^{\text{search}} + a_n^{i,j} T_{i,j+1}^{\text{search}}$$

END DO
DO $(j = 1, N_j)$
Solve for $T_{i,j}^{\text{search}}$ using TDMA: $a_{\text{p}}^{i,j} T_{i,j}^{\text{search}} = a_{\text{w}}^{i,j} T_{i-1,j}^{\text{search}} + a_{\text{e}}^{i,j} T_{i+1,j}^{\text{search}} + c_{i,j}$
END DO
END DO

Note that the first inner loop to evaluate $c_{i,j}$ is performed over *all* i, j before applying the TDMA. Combining the two inner loops can lead to poorer convergence.

Also note that no under-relaxation is used in the TDMA. Usually the line-by-line TDMA approach is done in alternate directions [12]. However, for the present problem only one direction as indicated above was enough. This is effective because the physical problem is roughly one-dimensional in the radial direction over much of the wire length.

2 Solve the minimum residual problem to update solution

First set

$$\left\{T'_{\text{search}}\right\} = \left\{T^{\text{search}}\right\} - \left\{T^{\text{current}}\right\}$$

Find x such that S is minimized:

$$S = \sum_{i,j} \left(r_{i,j} + x d_{i,j}\right)^2 \tag{A5}$$

where

$$\begin{aligned} d_{i,j} = a_{\text{w}}^{i,j} T'_{\text{search}}(i-1, j) + a_{\text{e}}^{i,j} T'_{\text{search}}(i+1, j) + a_{\text{s}}^{i,j} \\ \times T'_{\text{search}}(i, j-1) + a_{\text{n}}^{i,j} T'_{\text{search}}(i, j+1) - a_{\text{p}}^{i,j} T'_{\text{search}^{(i,j)}} \end{aligned}$$

If Eq. A5 is differentiated with respect to x, it is easy to show that

$$x = \frac{-\sum \left(r_{i,j} d_{i,j}\right)}{\sum \left(d_{i,j} d_{i,j}\right)}$$

The current solution is then updated using

$$\left\{T^{\text{current}}\right\} = \left\{T^{\text{current}}\right\} + x \left\{T'_{\text{search}}\right\} \tag{A6}$$

In concluding this section it is worth noting that it is extremely important that the solution to the discretized equations converges properly *every* time step. In the experience of the first author, most difficulties tend to occur during the first few time steps. When convergence difficulties occur, reducing the size of the time steps usually solves the problem. A failure to converge on just the first time step can destroy the accuracy of the method even if excellent convergence is achieved on all other time steps.

References

1. J.J. Healy, J.J. de Groot, J. Kestin, Physica **82C**, 392 (1976)
2. B. Taxis, K. Stephan, Int. J. Thermophys. **15**, 141 (1994)
3. H.M. Roder, R.A. Perkins, A. Laesecke, J. Res. Nat. Inst. Stand. Tech. **105**, 221 (2000)
4. M.J. Assael, S. Mixafendi, W.A. Wakeham, J. Phys. Chem. Ref. Data **15**, 1315 (1986)
5. M.J. Assael, L. Karagiannidis, N. Malamataris, W.A. Wakeham, Int. J. Thermophys. **19**, 379 (1998)
6. L. Sun, J.E.S. Venart, Int. J. Thermophys. **26**, 325 (2005)
7. G.C. Maitland, M. Mustafa, M. Ross, R.D. Trengove, W.A. Wakeham, M. Zalaf, Int. J. Thermophys. **7**, 245 (1986)
8. Y. Nagasaka, A. Nagashima, Rev. Sci. Instrum. **52**, 229 (1981)
9. M. Fujii, X. Zhang, N. Imaishi, S. Fujiwara, T. Sakamoto, Int. J. Thermophys. **18**, 327 (1997)
10. X. Zhang, W. Hendro, M. Fujii, T. Tomimura, N. Imaishi, Int. J. Thermophys. **23**, 1077 (2002)
11. X. Zhang, S. Fujiwara, Z. Qi, M. Fujii, J. Jpn. Soc. Micrograv. Appl. **16**, 129 (1999)
12. S.V. Patankar, *Numerical Heat Transfer and Fluid Flow* (Hemisphere, New York, 1980)
13. S.C. Eisenstat, H.C. Elman, M.H. Schultz, SIAM J. Numer. Anal. **20**, 345 (1983)

14. P. Wesseling, *Principles of Computational Fluid Dynamics* (Springer-Verlag, Berlin, 2001), pp. 273–276
15. J.M. Ortega, W. C. Rheinboldt, *Iterative Solution of Nonlinear Equations in Several Variables* (Academic Press, New York, 1970), pp. 267–269
16. L. Sun, J.E.S. Venart, R. C. Prasad, Int. J. Thermophys. **23**, 357 (2002)
17. NIST Standard Reference Database 69, June 2006 Release: NIST Chemistry WebBook, http://webbook.nist.gov/chemistry/
18. E.W. Lemmon, R.T. Jacobsen, Int. J. Thermophys **25**, 21 (2004)
19. Ch. Tegeler, R. Span, W. Wagner, J. Phys. Chem. Ref. Data **28**, 779 (1999)
20. M.L.V. Ramires, C.A. Nieto de Castro, R.A. Perkins, Y. Nagasaka, A. Nagashima, M.J. Assael, W.A. Wakeham, J. Phys. Chem. Ref. Data **29**, 133 (2000)
21. R.D. Goodwin, J. Phys. Chem. Ref. Data **18**, 1565 (1989)